Fermionized Photons in an Array of Driven Dissipative Nonlinear Cavities

I. Carusotto,[1,2] D. Gerace,[2,3] H. E. Tureci,[2] S. De Liberato,[4,5] C. Ciuti,[4] and A. Imamoğlu[2]

[1]*BEC-CNR-INFM and Dipartimento di Fisica, Università di Trento, I-38050 Povo, Italy*
[2]*Institute for Quantum Electronics, ETH Zürich, 8093 Zürich, Switzerland*
[3]*CNISM and Dipartimento di Fisica "A. Volta," Università di Pavia, 27100 Pavia, Italy*
[4]*Laboratoire Matériaux et Phénomènes Quantiques, Université Paris Diderot-Paris 7 and CNRS, UMR 7162, 75205 Paris Cedex 13, France*
[5]*Laboratoire Pierre Aigrain, École Normale Supérieure, 24 rue Lhomond, 75005 Paris, France*

(Received 22 December 2008; published 13 July 2009)

We theoretically investigate the optical response of a one-dimensional array of strongly nonlinear optical microcavities. When the optical nonlinearity is much larger than both losses and intercavity tunnel coupling, the nonequilibrium steady state of the system is reminiscent of a strongly correlated Tonks-Girardeau gas of impenetrable bosons. Signatures of strong correlations are identified in the transmission spectrum of the system, as well as in the intensity correlations of the transmitted light. Possible experimental implementations in state-of-the-art solid-state devices are discussed.

DOI: 10.1103/PhysRevLett.103.033601 PACS numbers: 42.50.Pq, 05.30.Jp, 05.70.Ln, 64.70.Tg

Strong correlations in quantum many-body systems give rise to a number of striking phenomena and states of matter, ranging from superfluidity of liquid helium and superconductivity of metals to the fractional quantum Hall effect in two-dimensional electron gases. Several recent papers have addressed quantum many-body aspects of gases of strongly interacting photons in suitably designed photonic structures [1]: e.g., the Mott insulator to superfluid transition in arrays of optical cavities [2], interacting spin models [3], the Tonks-Girardeau gas in a waveguide geometry [4], and quantum Hall states [5]. So far, most of the activity, however, focused on systems close to thermodynamic equilibrium, while the rich physics of nonequilibrium quantum many-body systems [6–8] remained largely unexplored. Given their intrinsically driven-dissipative nature [9], optical systems appear as most suitable candidates [10,11] to investigate the interplay of nonequilibrium and quantum many-body features.

In this Letter, we report the theoretical investigation of a genuine nonequilibrium state of strongly correlated photons. We study the observable signatures of strong interactions in an array of optical cavities mutually coupled by tunneling and driven by a coherent laser field. The properties of the nonequilibrium steady state are studied as a function of the pump frequency and intensity for a range of system parameters. Specific attention is devoted to the strongly nonlinear case, where nontrivial quantum correlations appear between photons indicating the onset of a Tonks-Girardeau gas of "fermionized photons." As the quantum correlations inside the many-cavity system directly transfer to the emitted radiation, a much wider range of observables is experimentally accessible than in analogous systems of ultracold atoms [12], and unambiguous qualitative signatures of photon fermionization can be identified in optical observables.

The system we consider is sketched in the left panel of Fig. 1: a closed and periodic necklace of M optical cavities coupled by nearest-neighbor photon tunneling, each displaying a sizable optical Kerr nonlinearity. All cavities are coherently driven by an incident laser beam. Assuming that the spacing between neighboring modes within a given cavity is much larger than all other energy scales, we can restrict our description to a single photon mode per cavity and write the system Hamiltonian in the following generalized single-band Bose-Hubbard form:

$$\mathcal{H} = \sum_i \hbar\omega_0 \hat{c}_i^\dagger \hat{c}_i + \hbar U \hat{c}_i^\dagger \hat{c}_i^\dagger \hat{c}_i \hat{c}_i - \sum_{\langle i,j\rangle} \hbar J \hat{c}_i^\dagger \hat{c}_j + \sum_i [\hbar F_i(t) \hat{c}_i^\dagger + \hbar F_i^*(t) \hat{c}_i]. \quad (1)$$

The $\hat{c}_i$ ($\hat{c}_i^\dagger$) operators destroy (create) a photon in the ith

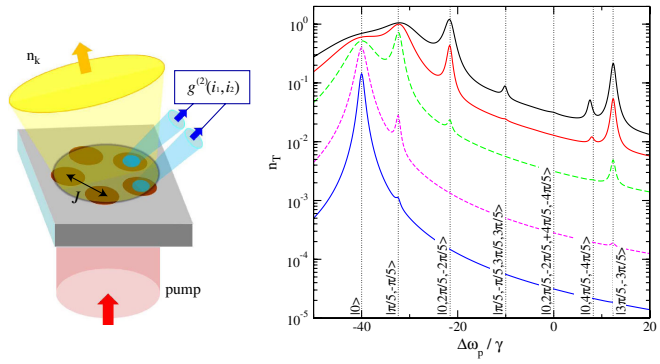

FIG. 1 (color online). Left panel: Sketch of the system under consideration. Right panel: Total transmission spectra as a function of the frequency $\Delta\omega_p = \omega_p - \omega_0$ of the pump beam. System of $M = 5$ cavities in the impenetrable boson limit $U/J = \infty$, with $J/\gamma = 20$. Different curves correspond to increasing values of the pump amplitude $F_p/\gamma = 0.1, 0.3, 1, 2, 3$. The vertical dotted lines indicate the spectral positions of the peaks predicted by the fermionization procedure.

cavity, and ω_0 is the bare frequency of the isolated cavities. $\langle i, j\rangle$ indicates next-neighbor cavities, and the intercavity hopping energy J can be quantitatively related to the spatial overlap of the modes of nearest-neighbor cavities [13]. The photon-photon interaction energy U arises from the Kerr optical nonlinearity of the underlying material. The term proportional to $F_i(t)$ accounts for the coherent drive of the ith cavity by the pump laser: In what follows, we will restrict our attention to the case of a monochromatic pump beam of frequency ω_p acting on all cavities with the same amplitude F_p, i.e., $F_i(t) = F_p \exp[-i\omega_p t]$. Photons are assumed to be lost from the system at a rate γ. The time evolution of the total density matrix $\rho(t)$ is then described by the master equation $d_t\rho = -\frac{i}{\hbar}[\mathcal{H}, \rho] + \frac{\gamma}{2}\sum_i(2\hat{c}_i\rho\hat{c}_i^\dagger - \hat{c}_i^\dagger\hat{c}_i\rho - \rho\hat{c}_i^\dagger\hat{c}_i)$.

In a configuration in which the pump light cannot directly propagate through the sample [15], information about the state of the system can be experimentally obtained by measuring the intensity and coherence properties of the transmitted light. The total transmitted intensity is proportional to the average total number of photons in the steady state $n_T = \sum_i\langle\hat{c}_i^\dagger\hat{c}_i\rangle$. The near-field pattern corresponds to the occupation $\hat{\rho}_i = \hat{c}_i^\dagger\hat{c}_i$ of each site, while the far-field one can be related to the momentum-space distribution $\hat{n}_k = \hat{b}_k^\dagger\hat{b}_k$, with $\hat{b}_k = \sum_j e^{-ikj}\hat{c}_j/\sqrt{M}$.

Let us start by discussing the eigenstates of the N boson problem in the absence of pumping and dissipation. In the linear regime $U = 0$, photons occupy single-particle states of the hopping Hamiltonian, with a dispersion $\epsilon(k) = \omega_0 - 2J\cos(k)$. Wave vector is defined here as a dimensionless quantity: The first Brillouin zone (FBZ) then corresponds to the interval $k \in [-\pi, \pi]$.

In the opposite limit of impenetrable bosons $U/J = \infty$, a generic bosonic N-body wave function $\psi(i_1 \ldots i_N)$ can be exactly mapped onto a fermionic one by the transformation [18]

$$\psi_F(i_1, \ldots, i_N) = \psi(i_1, \ldots, i_N)\epsilon(\sigma). \tag{2}$$

Here $i_1, \ldots, i_N$ are the positions of the N particles, σ is the permutation that sorts the spatial coordinates $i_1, \ldots, i_N$ into ascending order, and $\epsilon(\sigma)$ is the sign of the permutation σ. This sign guarantees that, for any wave function ψ symmetric under the exchange of any two particles, the corresponding ψ_F is antisymmetric as required by Fermi statistics.

As shown in Ref. [18], the eigenstates of the impenetrable boson problem are in a one-to-one correspondence with those of the noninteracting fermionic system, which are in turn simply classified by the occupation numbers of single-particle orbitals. In the following, we shall use the shorthand notation $|q_1 \ldots q_N\rangle$ to indicate the bosonic eigenstate corresponding to a Fermi wave function with one particle in each of the $q_1, \ldots, q_N$ orbitals. The (pseudo) momenta $q_{\alpha=1\ldots N}$ are to be chosen within the FBZ, i.e., $q_\alpha \in [-\pi, \pi]$. Both the energy and the *total* momentum of the bosonic state are equal to the ones of the corresponding fermionic one, say, $E = \sum_\alpha \epsilon(q_\alpha)$ and $P = \sum_\alpha q_\alpha$, respectively (as typical of a lattice, momentum is here defined only modulo 2π). On the other hand, the momentum distribution is not preserved by the Bose-Fermi mapping: The pseudomomenta q_α of the fermionic orbitals do not have a direct meaning in terms of physical observables of the bosonic particles and, in particular, do not correspond to their physical momentum k [18,19].

In our case of a periodic and closed necklace of M cavities, periodic boundary conditions have to be imposed on the bosonic N-body wave function, i.e., $\psi(\ldots, i_\alpha = 0, \ldots) = \psi(\ldots, i_\alpha = M, \ldots)$, $\forall\ \alpha$. A remarkable feature of the Bose-Fermi mapping is that the periodicity condition on ψ does not directly transfer to the single-particle orbitals of the fermionized wave function ψ_F: Depending on the number N of particles in the system, the fermionic orbitals have to fulfill either periodic (if N is odd) or antiperiodic (if N is even) boundary conditions [20,21]. This reflects on the quantization of the pseudomomentum $q = 2\pi n/M$ (if N is odd) or $q = 2\pi(n + 1/2)/M$ (if N is even), where n is an integer number. This peculiar quantization rule leads to the following explicit form of the bosonic wave function of the lowest $N = 2$ state $|q, -q\rangle$, with $q = \pi/M$ [18]:

$$\psi(i_1, i_2) = \frac{\sqrt{2}}{M}\sin\left[\frac{\pi}{M}|i_1 - i_2|\right]. \tag{3}$$

In contrast to equilibrium systems, pumping and losses induce transitions between states with a different number of photons: This suggests that detailed information on the microscopic physics of the strongly interacting photon gas can be extracted from the spectra of observable quantities as a function of the pump frequency ω_p and intensity. Examples of numerically calculated spectra of the total transmission are plotted in Fig. 1 for the case of impenetrable photons and weak loss rate $\gamma \ll J \ll U$.

For very weak driving $|F_p| \ll \gamma$, the dynamics is mostly restricted to the vacuum state and the $N = 1$, $|q = 0\rangle$ state of wave function $\psi(i_1) = 1/\sqrt{M}$: The resonant driving of this transition is responsible for the main peak that is visible in all spectra at $\Delta\omega_p = -2J$. For stronger driving amplitudes, $N > 1$ photon states start being excited by repeated absorption of N photons from the coherent drive. Provided the matrix element for the N-photon excitation process does not vanish by symmetry, a generic many-body state $|f\rangle$ of energy E_f then appears in the spectra as a resonance peak at frequency $\omega_p = E_f/N$. At low driving amplitudes, before power broadening effects set in [22], the intensity of a N-photon peak scales with the incident amplitude as $|F_p|^{2N}$. In the impenetrable boson limit considered in Fig. 1, the position of the numerical peaks successfully compares to the analytical predictions of the Bose-Fermi mapping indicated by the vertical lines: Each accessible N-photon state is associated to a set $q_{\alpha=1\ldots N}$ of pseudomomenta compatible with momentum conservation $P = \sum_\alpha q_\alpha \equiv 0[2\pi]$ and corresponds to a resonance peak at $\omega_p = \sum_\alpha \epsilon(q_\alpha)/N$.

In order to fully characterize the transition from the weakly to the strongly interacting regime, we have performed systematic numerical calculations for increasing values of the nonlinear coupling U/J (Fig. 2). The $M = 3$ case has been explored in full detail, and we have checked that our findings extend in a straightforward way to larger systems with more sites. Spectra of the population n_k in the $k = 0$ and $k = 2\pi/3$ modes are plotted in Figs. 2(a) and 2(b) for various values of U/J. Again, the main peak at $\Delta\omega_p = -2J$ corresponds to the resonance of the one-particle $|q = 0\rangle$ state [23]. The additional peak that splits from it as U/γ is increased corresponds to a two-particle state $|\psi_{N=2}\rangle$. The U/J dependence of its position and intensity [Figs. 2(c) and 2(d)] provides insight into its microscopic nature in the different regimes. Note that the two steps of the sequential decay $|\psi_{N=2}\rangle \rightarrow |-k\rangle \rightarrow |\mathrm{vac}\rangle$ contribute equally to n_k.

In the strong interaction regime ($U/J \gg 1$), the two-particle state is well captured by the lowest $N = 2$ fermionized state $|q, -q\rangle$, with $q = \pi/3$. This value of the pseudomomentum imposed by the antiperiodic boundary condition is a clear signature of the fermionization effect and directly reflects into the asymptotic position of the peak at $\Delta\omega_p/J = -2\cos(\pi/3) = -1$. The relative intensity of the peak on the different modes $n_{k=\pm 2\pi/3}/n_{k=0}$ is also in perfect agreement with the analytical predictions $n_{k=\pm 2\pi/3}/n_{k=0} = 1/4$ that are obtained by discrete Fourier transform of the wave function (3).

In the weakly interacting regime ($U/J \ll 1$), interactions can be treated within perturbation theory. To zeroth order in U/J, the lowest two-particle state is a factorizable bosonic state with two particles in the $k = 0$ mode and has an energy $-4J$. In this limit, it is visible only in the $k = 0$ spectrum as a peak at $\Delta\omega_p = -2J$. At the next order, the state energy is blueshifted by $2U/M$, and the wave function has the following analytical form:

$$\psi(i_1, i_2) \simeq \frac{1}{M}\left\{1 - \frac{2U}{9J}\cos\left[\frac{2\pi}{3}(i_1 - i_2)\right]\right\}. \qquad (4)$$

The hole around $i_1 = i_2$ that was complete in the fermionized wave function of the strong interaction limit (3) is here much less pronounced, and its depth scales as U/J. Correspondingly, the relative intensity of the peak at $\Delta\omega_p \simeq -2J + U/M$ on the $k = \pm 2\pi/3$ momentum components grows as $n_{k=\pm 2\pi/3}/n_{k=0} \simeq (U/9J)^2$. Note how the interaction-induced blueshift of the peak eventually saturates for large $U/J \gg 1$: The kinetic energy cost of creating a node at $i_1 = i_2$ is compensated by the suppressed interaction energy.

Further information on the microscopic nature of the many-body physics of the system can be obtained by inspecting the intensity correlations in the near-field transmission pattern $g^{(2)}(i_1, i_2) = \langle \hat{c}_{i_1}^\dagger \hat{c}_{i_2}^\dagger \hat{c}_{i_2} \hat{c}_{i_1} \rangle / \langle \hat{c}_{i_1}^\dagger \hat{c}_{i_1} \rangle \langle \hat{c}_{i_2}^\dagger \hat{c}_{i_2} \rangle$. Both the auto- ($i_1 = i_2$) and the cross ($i_1 \neq i_2$) correlations are plotted in Fig. 3 as a function of U/J for a pump laser kept exactly on resonance with the (U/J-dependent) two-photon transition.

In a very weakly interacting ($U/J \ll 1$) system, the resonance peaks corresponding to different values of N overlap, and the emitted light inherits the Poissonian nature of the pump laser. For intermediate values of $U/J \approx 1$, the two-particle peak is already well separated from the single-particle peak ($U/M \gg \gamma$). The resonant pump laser then selectively excites the two-particle state. The fact that the system preferentially contains $N = 0, 2$ particles rather than 1 is responsible for the strong bunching. The almost flat shape of the wave function (4) makes this bunching observable in both the auto- and the cross correlations of the emission. On the other hand, when interactions are very strong ($U/J \gg 1$) and the two-particle state has the fermionized form (3), the cross correlation remains strongly bunched, but the autocorrelation turns antibunched as a consequence of the strong on-site interactions [24].

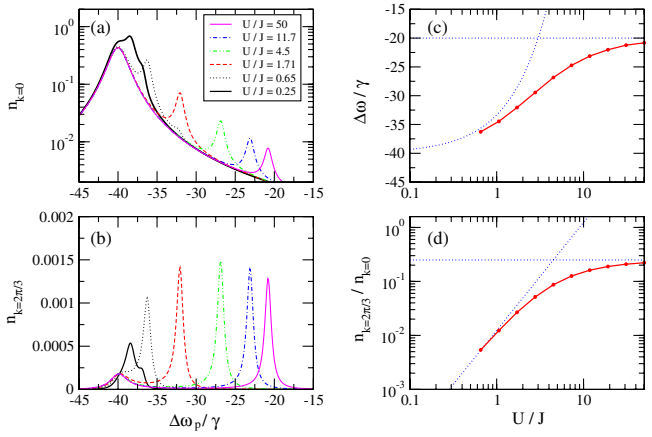

FIG. 2 (color online). (a),(b) Spectra of the population in the $k = 0$ and $k = 2\pi/3$ bosonic modes as a function of pump frequency for a fixed pump amplitude $F_p/\gamma = 0.5$ and different values of the nonlinear coupling U/J. (c),(d): Position of the peak and relative occupation $n_{k=2\pi/3}/n_{k=0}$ at the peak position as a function of U/J. The background signal due to the one-particle peak has been subtracted out from $n(k = 2\pi/3)$. Blue dashed lines: Asymptotic values in the weak $U/J \ll 1$ and strong $U/J \gg 1$ interaction limits. System of $M = 3$ cavities with $J/\gamma = 20$.

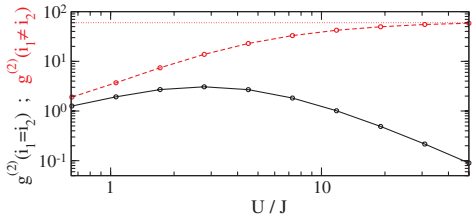

FIG. 3 (color online). Plot of the auto- (black, solid line) and cross- (red, dashed line) intensity correlations as a function of the interaction strength U/J. Red, dotted line: Analytical prediction for the cross-intensity correlation in the impenetrable boson limit. The same system parameters as in Fig. 2.

From the experimental point of view, the most challenging step is the integration of a strong nonlinearity [16,25,26] and an efficient intercavity tunneling [27,28]. Both aspects have been separately demonstrated in a number of cavity systems. Most promising candidates to our purpose are laterally patterned optical microcavities containing quantum wells as the nonlinear medium, e.g., micropillars [29] and polariton boxes [17,30]. Preliminary calculations [14] using the value of the polariton interaction constant inferred from available experiments suggest that the $U \gg \gamma$ polariton blockade regime should be achievable in polariton boxes [17] with a suitably tight optical confinement.

Another system of interest consists of superconducting stripline microwave cavities including Cooper-pair boxes as a nonlinear medium. While the recent demonstrations of photon blockade [31] and independent cavity tunability [32] strongly support the possibility of observing photon fermionization in a transmission spectrum, a direct observation of the quantum correlation effects in the emission still suffers from the current lack of efficient single microwave photon detectors [33].

In summary, we have theoretically investigated the spectroscopic signatures of a nonequilibrium, strongly correlated gas of photons in a driven-dissipative array of nonlinear cavities with strong photon-photon interactions. The imprint of the transition from the weakly to the strongly interacting regime has been discussed using readily accessible optical observables. We believe the present work demonstrates the importance of coupled nonlinear optical cavity systems in the theoretical and experimental investigation of quantum many-body systems out of equilibrium.

I. C. is grateful to J. Dalibard and Y. Castin for stimulating discussions at an early stage of the work. We acknowledge useful discussions with A. Badolato.

[1] M. H. Hartmann, F. G. S. Brandão, and M. B. Plenio, Laser Photon. Rev. **2**, 527 (2008).
[2] M. J. Hartmann, F. G. S. Brandao, and M. B. Plenio, Nature Phys. **2**, 849 (2006); A. D. Greentree, C. Tahan, J. H. Cole, and L. C. L. Hollenberg, Nature Phys. **2**, 856 (2006); D. G. Angelakis, M. F. Santos, and S. Bose, Phys. Rev. A **76**, 031805(R) (2007).
[3] M. J. Hartmann, F. G. S. L. Brandão, and M. B. Plenio, Phys. Rev. Lett. **99**, 160501 (2007).
[4] D. E. Chang *et al.*, Nature Phys. **4**, 884 (2008).
[5] J. Cho, D. G. Angelakis, and S. Bose, Phys. Rev. Lett. **101**, 246809 (2008).
[6] P. Werner, K. Völker, M. Troyer, and S. Chakravarty, Phys. Rev. Lett. **94**, 047201 (2005); T. Prosen and I. Pižorn, Phys. Rev. Lett. **101**, 105701 (2008).
[7] M. A. Zudov, R. R. Du, L. N. Pfeiffer, and K. W. West, Phys. Rev. Lett. **90**, 046807 (2003); R. G. Mani *et al.*, Nature (London) **420**, 646 (2002).
[8] C. Kollath, A. M. Läuchli, and E. Altman, Phys. Rev. Lett. **98**, 180601 (2007).
[9] D. Mukamel, arXiv:cond-mat/0003424; B. Schmittman and R. K. P. Zia, in *Statistical Mechanics of Driven Diffusive Systems*, edited by C. Domb and J. Lebowitz, Phase Transitions and Critical Phenomena Vol. 17 (Academic, New York, 1995).
[10] A. Amo *et al.*, Nature (London) **457**, 291 (2009); A. Amo *et al.*, arXiv:0812.2748.
[11] I. Carusotto and C. Ciuti, Phys. Rev. Lett. **93**, 166401 (2004); D. Gerace *et al.*, Nature Phys. **5**, 281 (2009).
[12] B. Paredes *et al.*, Nature (London) **429**, 277 (2004); T. Kinoshita, T. Wenger, and D. S. Weiss, Science **305**, 1125 (2004).
[13] A. Yariv, Y. Xu, R. K. Lee, and A. Scherer, Opt. Lett. **24**, 711 (1999).
[14] A. Verger, C. Ciuti, and I. Carusotto, Phys. Rev. B **73**, 193306 (2006).
[15] In contrast to photonic crystal cavities [16], this assumption is naturally fulfilled in systems of polariton boxes [17]: In this case, direct input light is in fact spectrally blocked by the distributed-Bragg-reflector mirrors, and all of the transmitted light originates from the cavities [14].
[16] K. Hennessy *et al.*, Nature (London) **445**, 896 (2007); A. Faraon *et al.*, Nature Phys. **4**, 859 (2008).
[17] O. El Daïf *et al.*, Appl. Phys. Lett. **88**, 061105 (2006); D. Lu *et al.*, Appl. Phys. Lett. **87**, 163105 (2005).
[18] M. D. Girardeau, J. Math. Phys. (N.Y.) **1**, 516 (1960).
[19] A. Lenard, J. Math. Phys. (N.Y.) **5**, 930 (1964).
[20] E. H. Lieb and W. Liniger, Phys. Rev. **130**, 1605 (1963).
[21] I. Carusotto and Y. Castin, New J. Phys. **5**, 91 (2003).
[22] Power broadening results in a dramatic broadening of the spectral lines as soon as the corresponding N-photon Rabi frequency is comparable to or larger than γ. This effect is easily visible on the strongest one-photon line at $\Delta\omega_p/\gamma = -40$ of Rabi frequency $\sqrt{M}F_p$.
[23] Despite the fact that the $N = 1$, $|q = 0\rangle$ state is a pure plane wave at $q = 0$, a resonance peak at $\Delta\omega_p/\gamma = -40$ is clearly visible in the $n_{k=2\pi/3}$ spectrum as well. Its physical origin can be traced back to an intermediate-state resonance in the two-photon excitation process to the $N = 2$, $|q, -q\rangle$ state.
[24] While the ratio $g^{(2)}(i_1 \neq i_2)/g^{(2)}(i_1 = i_2)$ depends only on the microscopic wave function of the $N = 2$, $|q, -q\rangle$ state, the absolute value of $g^{(2)}(i_1, i_2)$ depends on the pump amplitude. In particular, the analytic prediction for $g^{(2)}(i_1 \neq i_2)$ in the $U/J \gg 1$ limit scales as $|F_p|^{-2}$. These results include the two-photon excitation to the $N = 2$, $|q, -q\rangle$ state as well as the occupation of the $N = 1$ states from the decay of the $N = 2$ state and from direct nonresonant excitation of the $|q = 0\rangle$ state.
[25] K. M. Birnbaum *et al.*, Nature (London) **436**, 87 (2005).
[26] J. P. Reithmaier *et al.*, Nature (London) **432**, 197 (2004).
[27] A. Nakagawa, S. Ishii, and T. Baba, Appl. Phys. Lett. **86**, 041112 (2005); M. Benyoucef *et al.*, Phys. Rev. B **77**, 035108 (2008).
[28] T. D. Happ *et al.*, J. Opt. Soc. Am. B **20**, 373 (2003).
[29] D. Bajoni *et al.*, Phys. Rev. Lett. **100**, 047401 (2008).
[30] D. Sarchi, I. Carusotto, M. Wouters, and V. Savona, Phys. Rev. B **77**, 125324 (2008).
[31] A. Wallraff *et al.*, Nature (London) **431**, 162 (2004).
[32] M. Sandberg *et al.*, arXiv:0811.4449.
[33] G. Romero, J. J. García-Ripoll, and E. Solano, Phys. Rev. Lett. **102**, 173602 (2009).